Observation of supercontinuum generation in the direct simulation of an intense laser pulse propagating in a neutral gas

James Koga*

Advanced Photon Research Center, Japan Atomic Energy Research Institute, 8-1 Umemidai, Kizu, Kyoto 619-0215, Japan

(Received 7 November 2003; revised manuscript received 1 September 2004; published 11 November 2004)

The propagation of high power short pulse laser pulses in neutral gases is a surprisingly complex phenomenon. In order to study the detailed propagation dynamics a code has been developed which explicitly solves Maxwell's equations including the finite response time background neutral gas polarization and optical field ionization. In large scale two dimensional simulations of a high power laser pulse propagating in hydrogen-like gas the generation of ultrabroadband white light, the so-called supercontinuum generation, is observed.

DOI: 10.1103/PhysRevE.70.056404 PACS number(s): 52.38.−r, 42.65.Jx, 42.65.Sf, 52.35.Mw

Since the advent of high power short pulse lasers, there has been a renewed interest in the propagation dynamics of high power pulses in neutral gases [1]. A variety of interesting yet complex phenomena have been observed including the formation of long plasma channels in air [2–5] and the generation of ultrabroadband white light, the so-called supercontinuum generation, in a variety of neutral gases [6,7]. In our laboratory supercontinuum generation with a total blueshift of the laser pulse which is fixed and independent of the gas has also been observed [8]. The propagation of such laser pulses is complex and therefore simulation is necessary. A variety of simulations have been performed to study these phenomena. Sophisticated simulations have shown that the propagation dynamics of the laser pulse are turbulent in nature [9]. Additionally, in similar types of simulations the supercontinuum radiation has been reproduced in the envelope approximation [10–12] and in the unidirectional optical pulse propagation approximation [13]. In order to study these types of problems with a minimal amount of approximation we have developed a nonlinear polarization ionization code (NOPIC). In NOPIC we explicitly solve in two dimensions Maxwell's equations, the background neutral gas polarization, and optical field ionization by the laser pulse. The advantage of this method is that fewer approximations are made than with envelope solutions such as the nonlinear Schrödinger equation or unidirectional propagation solutions where backscattered radiation is assumed to be weak [13]. The disadvantage is that much higher resolution in space and time is necessary. This can be somewhat overcome by using massively parallel computers. In this paper we describe the numerical model equations and present results of supercontinuum generation by a high power laser pulse propagating in a neutral gas. Supercontinuum generation is observed in the direct solution of Maxwell's equations without envelope or unidirectional propagation approximations.

Maxwell's equations including source terms from the plasma and polarization effects of the background gas can be written as [14]

$$\frac{\partial^2 \vec{E}}{\partial t^2} - c^2 \nabla^2 \vec{E} = -4\pi \left(\frac{\partial \vec{J}}{\partial t} + \frac{\partial^2 \vec{P}}{\partial t^2} \right), \tag{1}$$

where $\vec{E}$ is the electric field of the laser pulse, $\vec{J}$ is the current, and $\vec{P}$ is the polarization of the background gas. The contribution of plasma is through the current and including weak relativistic effects is of the form [14]

$$\frac{\partial \vec{J}}{\partial t} = \frac{q^2 n_e}{m_e} (1 + a^2)^{-1/2} \vec{E}, \tag{2}$$

where q is the charge, n_e is the electron plasma density, m_e is the electron mass, and $a = e|\vec{E}|/m_e c\omega$ is the unitless laser strength parameter in which ω is the laser frequency. The polarization equation can be written in the form [15]

$$\frac{\partial^2 \vec{P}}{\partial t^2} + \frac{q^5 n_N^3}{m_e} \frac{\vec{P}}{(P_0^2 + P^2)^{3/2}} + \Gamma \frac{\partial \vec{P}}{\partial t} = \frac{q^2 n_N}{m_e} \vec{E}, \tag{3}$$

where $P_0 = n_N q a_0$, $\vec{P} = n_N q \vec{x}$, $\vec{x}$ is the displacement from equilibrium of the bound electrons, and n_N is the neutral density of the gas. Typically, $\vec{E}$ varies on slower time scales than $\vec{P}$. $\vec{P}$ is a function of the form $\vec{P}(\vec{x}, t)$. We have assumed a soft-core potential for the atomic response with equilibrium radius a_0 which is of the order of the Bohr radius [16]. By using this the polarization finite response time and saturation of the gas are automatically included. Plasma formation is taken into account by [17]

$$\frac{\partial n_e}{\partial t} = (n_{N0} - n_e) W(|\vec{E}|), \tag{4}$$

where n_{N0} is the initial neutral density and the term W is the optical field ionization rate given by [18]

$$W(|\vec{E}|) = 4\omega_a \left(\frac{\epsilon_i}{\epsilon_h} \right)^{5/2} \frac{E_a}{|\vec{E}|} \exp\left[-\frac{2}{3} \left(\frac{\epsilon_i}{\epsilon_h} \right)^{3/2} \frac{E_a}{|\vec{E}|} \right], \tag{5}$$

where $\omega_a = m_e e^4/\hbar^3$, $E_a = m_e^2 e^5/\hbar^4$, ϵ_h and ϵ_i are the ionization potentials of hydrogen and the atom under consideration.

Equations (1)–(3) are finite differenced in space and time on a two dimensional Cartesian grid and are time centered. The code has been parallized using a two dimensional do-

*Electronic address: koga@apr.jaeri.go.jp

main decomposition with inter-CPU communication using MPI. The code was run on the Hewlett-Packard AlphaServer SC ES40 using 720 CPU's. The size of the integration time step is limited by the polarization equation [Eq. (3)] and ionization equation [Eq. (5)], since the fastest oscillations occur there. The oscillation frequency ω_R can be estimated from Eq. (3) by assuming that $|P| \ll P_0$:

$$\omega_R = \sqrt{\frac{q^2}{m_e a_0^3}}. \tag{6}$$

The maximum ionization rate can be calculated from Eq. (5) $W_{max} = 6e^{-1}\omega_a$. The time step Δt should be chosen so that $\omega_R \Delta t < 1$ and $W_{max}\Delta t < 1$.

We performed two dimensional simulations of the propagation of a 1-μm wavelength 26 GW linearly polarized laser pulse propagating in a hydrogenlike neutral gas at 1000 times atmospheric pressure (2.7×10^{22} cm^{-3}). This high density was chosen so that the self-focusing effects take place over a short distance. The pulse was temporally and spatially Gaussian with a duration of 266 fs and spot size of 200 μm. In order to avoid transient oscillations the pulse was propagated from a low neutral density region into the high neutral density region via a hyperbolic tangent ramp of length 20 μm. The pulse is initially weakly focused so that it is 10% of the Rayleigh distance away from the focus point assuming Gaussian pulse propagation. This was done to compensate for any defocusing that might occur due to the neutral density ramp. The wavelength of the laser was resolved by ten grid cells so that the total simulation box size was 4000 by 18 000 grids in the x and y directions where x is the propagation direction. The boundaries were periodic in y and absorbing in x [19]. The soft core radius a_0 was set to be 1.5 Bohr radii. The resulting depth of the soft core potential well is 18.1 eV which is comparable to the ionization level of 13.6 eV for hydrogen which was chosen for ϵ_i. The initial pulse intensity is 1.7×10^{13} W/cm^2 which is far below the threshold ionization intensity of 1.4×10^{14} W/cm^2. The charge was set so that $q = e$, resultingly, $\omega_R/\omega = 11.9$ and $W_{max}/\omega = 48.4$. The simulation time step was chosen so that $\omega \Delta t = 0.006$.

The critical power for self-focusing is given by [20]

$$P_{cr} = \frac{\pi (0.61)^2 \lambda^2}{8 n_0 n_2}, \tag{7}$$

where λ is the laser wavelength, n_0 is the linear index of refraction, and n_2 is the nonlinear index of refraction. The indices of refraction can be calculated from the Taylor series expansion of the soft core potential [15]:

$$n_0 = \sqrt{1 + 4\pi a_0^3 n_N}, \tag{8}$$

$$n_2 = \frac{576\pi^2}{n_0^2 c} \frac{a_0^7 n_N}{q^2}. \tag{9}$$

Using these formulas we find that $P/P_{cr} = 308$ where P is the power of the laser pulse. This implies that the pulse should easily self-focus. The self-focusing distance z_f is calculated to be 0.8 cm [20]. The previous estimate is for the whole beam to focus. Small scale focusing including background saturation occurs over shorter distances and is given by [3]

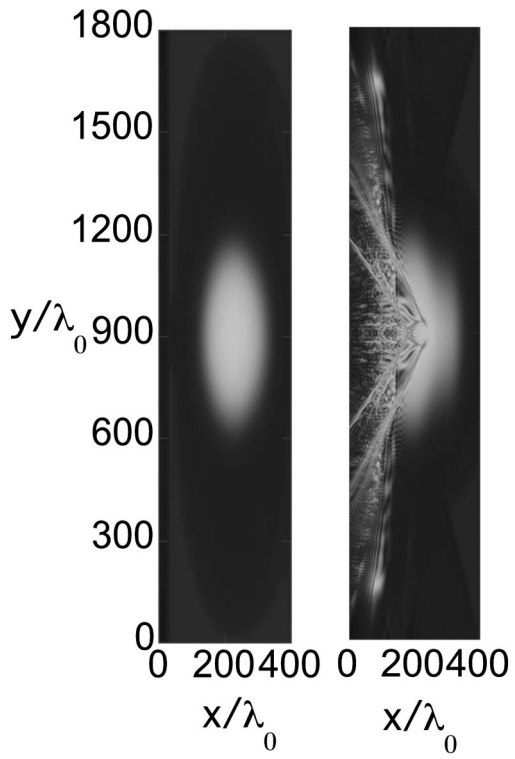

FIG. 1. Laser field after propagating 200 μm (left) which is past the neutral density ramp and after propagating 0.5 cm (right) in the neutral gas.

$$z_f = \frac{\lambda}{2\pi n_2 I_0} \ln\left(1 + \frac{\sqrt{2}}{\delta}\right), \tag{10}$$

where I_0 is the initial maximum intensity and δ is the initial modulation depth of the laser pulse. This focusing distance is closer to that observed experimentally [3]. Using this formula we get 0.16 cm with $\delta = 0.1$.

Figure 1 shows the laser pulse after it has propagated 200 μm (left) which is past the neutral density ramp and after propagating 0.5 cm (right) in the gas. The simulation box is moving with the laser pulse at nearly the speed of light. We can see that the back of the laser pulse has been strongly modified. This is what has been previously referred to as an optical shock at the back of the pulse [21]. This shock has been proposed as the source of the supercontinuum generation [21]. The effective spot size of the laser pulse has increased by a factor of 2. All fields are below the theoretical ionization threshold field.

Figure 2 shows a zoom up of the central region of the laser pulse. We can see that a very complex structure has formed in the back of the pulse. Many filaments of various sizes have formed. The filament sizes are predicted to be [22]

$$d = \frac{\lambda}{4\sqrt{n_2 I_{crit}}}, \tag{11}$$

where I_{crit} is the critical threshold ionization intensity of the gas. From the simulation paramters the filament size is predicted to be 5.4 μm.

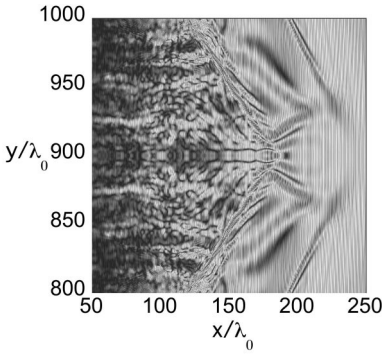

FIG. 2. Zoom up of the laser field after propagating 0.5 cm in neutral gas.

Figure 3 shows the power spectrum of the laser pulse taken in the y direction and the spectrum averaged over x (white line). Towards the back of the pulse there is a broad spectrum of filament sizes. In the figure we can see a peak in the spectrum for k/k_0 of about 0.2 which corresponds to the predicted filament size. From the figure it can be seen that the place where the filament sizes are close to theory occur between $50 < x/\lambda_0 < 100$.

At the same propagation distance Fig. 4 shows the corresponding plasma formation in the laser pulse. We can see that plasma filaments have formed. Down the center of the pulse the filaments are straight lines. However, at the edges of the pulse the structure is more complicated.

The equilibrium plasma density n_p can be estimated by assuming that sustained channeling of the laser pulse occurs [23]:

$$n_2 I_{crit} = \frac{\omega_p^2}{2\omega^2} + \frac{(1.22\lambda)^2}{8 n_0 \pi w_0^2}, \tag{12}$$

where $\omega_p = \sqrt{4\pi e^2 n_p / m_e}$ is the plasma frequency and w_0 is the initial laser spot size. In Eq. (12) the left hand side refers to the self-focusing, the first term on the right hand side refers to plasma diffraction, and the second term on the right hand side refers to vacuum diffraction. From this equation one can calculate the balance plasma density, since $\omega_p^2/2\omega^2$ is $n_p/2n_c$ where n_c is the critical density,

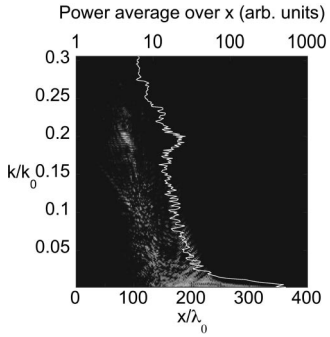

FIG. 3. Power spectrum in the direction transverse (y) to the propagation of the laser field after propagating 0.5 cm in neutral gas and the spectrum averaged over the propagation direction (x) (white line).

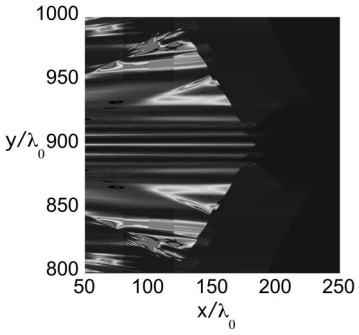

FIG. 4. Zoom up of the plasma after the laser has propagated 0.5 cm in neutral gas.

$$\frac{n_p}{n_c} = 2\left(n_2 I_{crit} - \frac{(1.22\lambda)^2}{8 n_0 \pi w_0^2} \right). \tag{13}$$

Using the parameters from the simulation we get $n_p/n_c = 4.3 \times 10^{-3}$. The plasma density near the center of the pulse ($875 < y/\lambda_0 < 925$) is found to be close to the theoretical prediction. Exactly down the center ($y/\lambda_0 = 900$) the density is about a factor of 2 higher than the theoretical value, however, at the edges of the pulse ($y/\lambda_0 \leqslant 850$ and $y/\lambda_0 \geqslant 950$) the density reaches very high values. Some points exceed critical density.

Figure 5 shows power spectra of the laser pulse taken in the x direction averaged over y. One can see that as the laser pulse propagates in the neutral gas, supercontinuum generation is observed with a spectral dropoff which is similar to experiments [6,7]. The initial laser pulse is centered around $\lambda/\lambda_0 = 1$. There is a shift in the spectrum as the laser pulse propagates from the low density region to the high density region of the simulation from the increase in the index of refraction. The shift can be calculated using Eq. (8) and $\lambda/\lambda_0 = 1/n_0$ to get $\lambda/\lambda_0 = 0.92$. After reaching the high density region the spectrum begins to spread. The spread reaches wavelengths as short as $\lambda/\lambda_0 \approx 0.5$.

Figure 6 shows the power spectrum as a function of the wave number k normalized by the initial wave number k_0 and y where the amplitude is log scale after the pulse has propagated 0.5 cm. We can see that the short wavelength components occur transversely near the center of the pulse. The shortest wavelengths occur slightly off the center of the

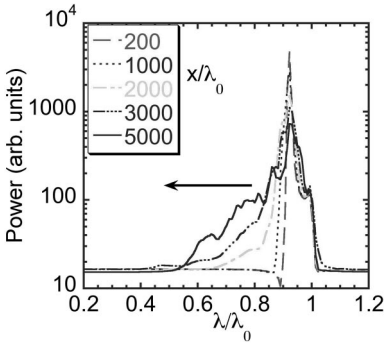

FIG. 5. Power spectra in the propagation direction (x) of the laser pulse as a function of propagation distance in the gas.

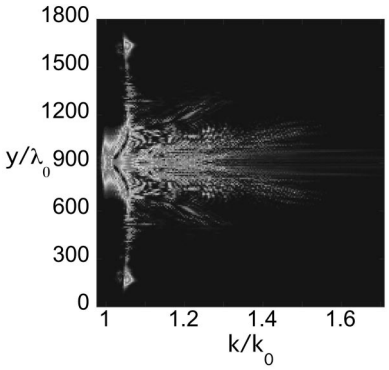

FIG. 6. Two dimensional spectrum as a function of wave number k normalized by the initial wave number k_0 and y where the amplitude is log scale.

pulse. The source of this broadening is still under investigation, but is most likely due to the complex interaction of the laser filaments and plasma formation. We have speculated that this complex interaction is a self-organized critical state [24].

In order to determine the effects of the nonlinearity in the polarization in Eq. (3) a simulation with the same parameters was run with a linear polarization response:

$$\frac{\partial^2 \vec{P}}{\partial t^2} + \frac{q^5 n_N^3}{m_e} \frac{\vec{P}}{P_0^3} + \Gamma \frac{\partial \vec{P}}{\partial t} = \frac{q^2 n_N}{m_e} \vec{E}. \tag{14}$$

Figure 7 shows power spectra of the laser pulse for the nonlinear (solid line) and linear (dashed line) response taken in the x direction averaged over y after the pulse has propagated 0.5 cm. We can see that the spectrum is broader in the case with the nonlinear response. The spectrum from the linear response is found to remain the same after propagating 0.3 cm. The spead reaches wavelengths as short as $\lambda/\lambda_0 > 0.6$.

The largest difference in spectra appear in the direction transverse to the propagation direction. Figure 8 shows the power spectrum of the laser pulse as a function of the wave number k normalized by the initial wave number k_0 for the nonlinear (solid line) and linear (dashed line) response taken

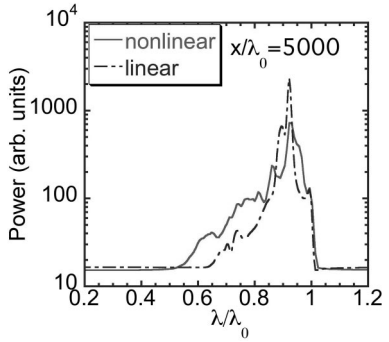

FIG. 7. Comparison of the power spectra in the propagation direction (x) averaged over the transverse direction (y) of the laser pulse after propagating 0.5 cm in neutral gas with nonlinear (solid line) and linear (dashed line) response.

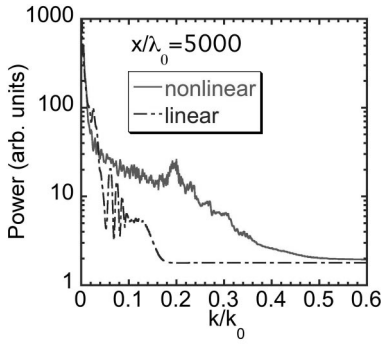

FIG. 8. Comparison of the power spectra in the transverse direction (y) averaged over the propagation direction (x) of the laser pulse with nonlinear (solid line) and linear (dashed line) response after propagating 0.5 cm in the gas. The spectra are functions of wave number k normalized by the initial wave number k_0.

in the y direction averaged over x after the pulse has propagated 0.5 cm. The peak at $k/k_0 = 0.2$ due to filament formation seen in the nonlinear response case is not seen in the linear response case. This is due to the fact that the nonlinear focusing and filament formation do not occur in the linear response case. It can be seen that the case with nonlinear response is significantly broader than in the linear response case. Due to the complex interaction of filaments transverse perturbations are driven to scales as small as twice the original wavelength $k/k_0 \approx 0.5$.

The results from our simulations indicate that the slow envelope approximation, as expected, is pretty good at predicting the overall propagation characteristics of the laser pulse. Theoretical predictions based on envelope approximations are found to be in good agreement with the simulations. For example, the dominant transverse filament size is found to agree well with theoretical predictions based on envelope approximations [22]. In addition, the predicted balance density is also in good agreement with theory along the center of the pulse [23]. The simulations also generate the overall shape of the supercontinuum spectra observed in simulations based on the envelope approximation [10–12]. Although detailed comparison with slow envelope approximation numerical solutions is outside the scope of the current paper, we expect that differences should occur in the details of the pulse propagation at the edges of the pulse and at wavelengths shorter than the carrier wave where application of the paraxial approximation used in the slow wave approximation is expected to be limited. Examples from the simulations include the observation of high plasma densities at the edges of the pulse where the amount of reflected light can become large, the details in the power spectra in Fig. 5 showing wavelengths shorter than the carrier wavelength, and the scattering of parts of the laser pulse to large angles as seen in Fig. 1 after propagating 0.5 cm. In addition, large deviations are expected from the slow envelope approximation when we go to subcycle laser pulses where the approximation breaks down.

In conclusion we have performed a large scale direct solution of Maxwell's equations with finite response time gas

polarization and optical field ionization of the propagation of high power laser pulses in neutral gas. We have reproduced supercontinuum generation without envelope or unidirectional propagation approximations. The nonlinear polarization response of the gas which leads to self-focusing and plasma formation is found to drive a broad range of transverse perturbations. The transverse perturbation scale lengths are as small as twice the original laser wavelength. In the next paper the complex interaction between the laser field, generated plasma, and neutral gas response will be further analyzed. In addition we will study ultrashort subcycle laser pulse propagation.

We wish to acknowledge fruitful comments and suggestions from Y. Kishimoto, H. Kotaki, T. Utsumi, A. Zhidkov, S. V. Bulanov, T. Esirkepov, M. Yamagiwa, and T. Tajima.

[1] A. L. Gaeta, Science **301**, 54 (2003).
[2] A. Braun, G. Korn, X. Liu, D. Du, J. Squier, and G. Mourou, Opt. Lett. **20**, 73 (1995).
[3] A. Braun, Ph.D. thesis, The University of Michigan, 1997.
[4] A. Brodeur, C. Y. Chien, F. A. Ilkov, S. L. Chin, O. G. Kosareva, and V. P. Kandidov, Opt. Lett. **22**, 304 (1997).
[5] H. R. Lange, G. Grillon, J.-F. Ripoche, M. A. Franco, B. Lamouroux, B. S. Prade, A. Mysyrowicz, E. T. J. Nibbering, and A. Chiron, Opt. Lett. **23**, 120 (1998).
[6] P. B. Corkum, C. Rolland, and T. Srinivasan-Rao, Phys. Rev. Lett. **57**, 2268 (1986).
[7] H. Nishioka, W. Odajima, K. Ueda, and H. Takuma, Opt. Lett. **20**, 2505 (1995).
[8] J. K. Koga, N. Naumova, M. Kando, L. N. Tsintsadze, K. Nakajima, S. V. Bulanov, H. Dewa, H. Kotaki, and T. Tajima, Phys. Plasmas **7**, 5223 (2000).
[9] M. Mlejnek, M. Kolesik, J. V. Moloney, and E. M. Wright, Phys. Rev. Lett. **83**, 2938 (1999).
[10] N. Aközbek, M. Scalora, C. M. Bowden, and S. L. Chin, Opt. Commun. **191**, 353 (2001).
[11] M. Kolesik, G. Katona, J. V. Moloney, and E. M. Wright, Appl. Phys. B: Lasers Opt. **77**, 185 (2003).
[12] M. Kolesik, G. Katona, J. V. Moloney, and E. M. Wright, Phys. Rev. Lett. **91**, 043905 (2003).
[13] M. Kolesik, J. V. Moloney, and M. Mlejnek, Phys. Rev. Lett. **89**, 283902 (2002).
[14] P. Sprangle, E. Esarey, and J. Krall, Phys. Rev. E **54**, 4211 (1996).
[15] J. Koga, Opt. Lett. **24**, 408 (1999).
[16] J. H. Eberly, J. Javanainen, and K. Rzążwski, Phys. Rep. **204**, 331 (1991).
[17] X. Liu and D. Umstadter, in *OSA Proceedings on Shortwavelength V*, edited by P. B. Corkum and M. D. Perry, 1993, Vol. 17, p. 45.
[18] L. D. Landau and E. M. Lifshitz, *Quantum Mechanics* (Butterworth-Heinemann, Oxford, 1997).
[19] E. L. Lindman, J. Comput. Phys. **18**, 66 (1975).
[20] R. W. Boyd, *Nonlinear Optics* (Academic, San Diego, 1992).
[21] A. L. Gaeta, Phys. Rev. Lett. **84**, 3582 (2000).
[22] N. C. Kothari and T. Kobayashi, Phys. Rev. Lett. **50**, 160 (1983).
[23] A. Javan and P. L. Kelley, IEEE J. Quantum Electron. **QE-2**, 470 (1966).
[24] J. Koga, in ISPJ Symposium Series, edited by E. Tomita and M. Miki, 2000, Vol. 2000, p. 109.